

EXPRESS LETTER

Structure-Spin-Transport Anomaly in Quasi-One-Dimensional $\text{Ba}_9\text{Fe}_3\text{Te}_{15}$ under High Pressure

To cite this article: Jun Zhang *et al* 2020 *Chinese Phys. Lett.* **37** 087106

View the [article online](#) for updates and enhancements.

中国物理快报
Chinese Physics
Letters

CLICK HERE
for our
Express Letters

Structure-Spin-Transport Anomaly in Quasi-One-Dimensional $\text{Ba}_9\text{Fe}_3\text{Te}_{15}$ under High Pressure

HPSTAR
980-2020

Jun Zhang(张俊)^{1,2,3†}, Mei-Ling Jin(金美玲)^{1,8†}, Xiang Li(李翔)^{4†}, Xian-Cheng Wang(望贤成)^{2*}, Jian-Fa Zhao(赵建发)^{2,3}, Ying Liu(刘影)⁵, Lei Duan(段磊)^{2,3}, Wen-Min Li(李文敏)^{2,3}, Li-Peng Cao(曹立朋)², Bi-Juan Chen(陈碧娟)¹, Li-Juan Wang(王丽娟)¹, Fei Sun(孙菲)¹, Yong-Gang Wang(王永刚)¹, Liu-Xiang Yang(杨留响)¹, Yu-Ming Xiao(肖玉明)⁶, Zheng Deng(邓正)², Shao-Min Feng(冯少敏)², Chang-Qing Jin(靳常青)^{2,3,7*}, and Jin-Long Zhu(朱金龙)^{1,8*}

¹Center for High Pressure Science & Technology Advanced Research, Beijing 100094, China

²Beijing National Laboratory for Condensed Matter Physics, Institute of Physics, Chinese Academy of Sciences, Beijing 100190, China

³School of Physics, University of Chinese Academy of Sciences, Beijing 100190, China

⁴Key Laboratory of Advanced Optoelectronic Quantum Architecture and Measurement (Ministry of Education), School of Physics, Beijing Institute of Technology, Beijing 100081, China

⁵Xi'an Modern Chemistry Research Institute, Xi'an 710065, China

⁶High Pressure Collaborative Access Team (HPCAT), Advanced Photon Source, Argonne National Laboratory, Argonne, Illinois 60439, USA

⁷Songshan Lake Materials Laboratory, Dongguan 523808, China

⁸Department of Physics, Southern University of Science and Technology, Shenzhen 518055, China

(Received 22 June 2020; accepted 16 July 2020; published online 19 July 2020)

Recently, a series of novel compounds Ba_3MX_5 ($M = \text{Fe, Ti, V}$; $X = \text{Se, Te}$) with hexagonal crystal structures composed of quasi-1-dimensional (1D) magnetic chains has been synthesized by our research team using high-pressure and high-temperature methods. The initial hexagonal phases persist to the maximum achievable pressure, while spin configurations and magnetic interactions may change dramatically as a result of considerable reductions in interchain separations upon pressurization. These compounds therefore offer unique possibilities for studying the evolution of intrinsic electronic structures in quasi-1D magnetic systems. Here we present a systematic investigation of $\text{Ba}_9\text{Fe}_3\text{Te}_{15}$, in which the interchain separations between trimerized 1D chains ($\sim 10.2 \text{ \AA}$) can be effectively modulated by external high pressure. The crystal structure especially along the 1D chains exhibits an abnormal expansion at $\sim 5 \text{ GPa}$, which accompanies trimerization entangled anomalous mixed-high-low spin transition. An insulator-metal transition has been observed under high pressure as a result of charge-transfer gap closing. Pressure-induced superconductivity emerges at 26 GPa , where the charge-transfer gap fully closes, 3D electronic configuration forms and local spin fully collapses.

PACS: 71.27.+a, 71.30.+h, 74.62.Fj

DOI: 10.1088/0256-307X/37/8/087106

High-pressure-driven lattice distortions, spin fluctuations and relevant electronic interactions can induce quantum phase transitions and therefore disclose the fundamental mechanism of quantum parameter competitions.^[1–2] A system with quasi 1-dimensional (1D) spin chains is expected to display rich quantum phenomena^[3] due to the coexistence of strong electro-phonon couplings and electron-electron interactions, such as spin-Peierls transitions^[4] and field-induced quantum phenomena.^[5] Moreover, a 1D system with magnetism has strong jj exchange interactions along the 1D-chain direction but much weaker ones normal to the chain. Ba_3TiTe_5 is a typical 1D conductor exhibiting semiconducting behavior due to Umklapp scattering, and gradually changed to 3D metal with emerging superconductivity under high

pressure.^[5] Specifically, due to the dimerization or trimerization, hexagonal Ba_3MX_5 ($M = \text{Fe, Ti, V, Cr}$; $X = \text{S, Se, Te}$)^[5–9] systems show complex geometric modulated spin interactions, therefore exhibit rich macroscopic properties. For instance, our previous study shows that dimerized $\text{Ba}_6\text{Cr}_2\text{S}_{10}$ exhibits a rare ferrotoroidicity with 1D spin chain.^[6] Another example is that $\text{Ba}_9\text{V}_3\text{Se}_{15}$ ^[8] is a ferrimagnetic insulator with a distance of adjacent iron chains being 9.6 \AA . The large magnetic frustration coefficient of 12.4 proves its better 1D structure. It is believed that the increase of interaction between the adjacent vanadium chains imposes an important influence on the electronic transport and magnetic property. Substitution of V by Fe, trimerized $\text{Ba}_9\text{Fe}_3\text{Se}_{15}$ hosts multiferroicity with a conical spin arrangement along the

Supported by the National Natural Science Foundation of China (Grant Nos. U1930401, 11974410, 11820101003, 11921004 and 11534016), and the National Key R&D Program of China (Grant Nos. 2018YFA0305703, 2018YFA0305700 and 2017YFA0302900).

[†]These authors contributed equally to this work.

*Corresponding authors. Email: wangxiancheng@iphy.ac.cn; jin@iphy.ac.cn; zhujl@sustech.edu.cn

© 2020 Chinese Physical Society and IOP Publishing Ltd

c axis.^[9]

Generally, the examination of these 1D characters and their evolution through manipulating chains distance by family elemental substitution or compression is of special interest in aspect of spintronic modulation.^[10] Moreover, the strong magnetic interaction anisotropy in a 1D system can be effectively tuned by extra parameters, such as temperature, magnetic field, chemical doping, as well as high pressure. Quasi-1D BaVS₃ with an interchain of 6.7 Å exhibits incommensurate antiferromagnetic order (ICAFO) transition at $T_N \sim 31$ K.^[11–12] Enhancing the chain interactions, either by chemical pressure exerted by Sr-doping^[13] or in the presence of sulfur deficiency larger than 0.05,^[14] can suppress ICAFO and further lead to the ferromagnetic state; and a metal-insulator transition at ~ 69 K driven by charge density order in quasi-1D BaVS₃ can also be tuned to be complete metallic state when pressure is applied higher than 2 GPa.^[15–16] Another intriguing quantum phenomenon is that superconductivity could be induced in these 1D compounds, as similar with pressure induced superconductivity in the two-leg spin ladder 123-type iron chalcogenides BaFe₂Se₃^[17–18] and BaFe₂Se₃.^[19] Our previous results show that Ba₉Fe₃Se₁₅ is antiferromagnetic with T_N at 14.5 K,^[9] and no superconducting transition is realized with pressure up to 60 GPa. To further suppress the magnetic interaction and inducing non-magnetic transition, hence producing possible unconventional magnetically-mediated superconductivity in this 1D spin chain system, substitution of Se by Te in Ba₉Fe₃Se₁₅ is proposed, as the larger radius of Te ions can effectively suppress magnetic interaction of neighbored Fe ions.

Here high-pressure quenched meta-stable quasi-1D Ba₉Fe₃Te₁₅ was investigated through *in-situ* synchrotron diffraction, x-ray emission scattering (XES), and transport measurements as a function of pressure. In the whole pressure range studied, the hexagonal structure is robust, which provides us an ideal framework to study the evolution of electronic structure. In this “rigid” structure, we demonstrated Fe²⁺ spin fluctuations occurring in the pressure range from ~ 2 GPa to 10 GPa, accompanied by an insulator-to-metal transition (MIT). The MIT is driven by an increase of the Fe 3*d* and Te 5*p* electrons hybridization under pressure. A full metallization achieved at ~ 26 GPa suggests the closure of charge-transfer gap related to a complete 1D-to-3D framed electronic transition. More importantly, the Ba₉Fe₃Te₁₅ system shows a rare pressure-driven mixed-spin to high-spin transition, reentrance of spin state at ~ 5.5 GPa, which can be ascribed to the anomalous structural and transport characteristics.

Ba₉Fe₃Te₁₅ polycrystalline samples were synthesized by employing a solid state reaction under high-pressure and high-temperature conditions.^[7] High-

pressure synchrotron x-ray diffraction experiments were performed at 16 BMD, HPCAT of the Argonne National Laboratory with a wavelength of 0.4246 Å at room temperature in a symmetric diamond anvil cell (DAC) with a culet at 300 μm in diameter. A T301 steel gasket was pre-indented from 250 μm to 40 μm, and a central hole with diameter of 150 μm was drilled. The hole was compressed to 120 μm with neon loaded as a nearly hydrostatic pressure transmitting medium. Ruby balls were placed near the sample as pressure markers. The x-ray diffraction patterns were collected with an MAR 3450 image plate detector. The obtained 2D image plate patterns were converted to 1D 2θ versus intensity data utilizing the Fit 2D software package. Refinements of x-ray diffraction patterns are performed by applying the GSAS + EXPGUI/GSAS II software packages.^[20] The refined results display that the lattice volume decreases monotonously by 30.6% with pressure increasing from ambient to 40 GPa and the lattice parameters of a and c exhibit anisotropic compression, i.e., decreased by 10.9% for a and by 12.0% for c . For the high-pressure XES experiments, Be gaskets were used as a sample chamber and neon gas was used as a pressure-transmitting medium. The quantitative analysis of XES data allows us to detect the change of spin numbers with increasing pressure, which is proportional to the changes of local magnetic moments. According to the procedure described by Vankó *et al.*,^[21] the spectra were normalized firstly with respect to the areas and then shifted to centers of mass at the same position. The integrals of the absolute values of different spectra (IAD) were obtained by subtracting low-spin values from high-spin values. The Fe²⁺ in Ba₉Fe₃Te₁₅ at ambient pressure is mixed spin state (IAD = 0.11). As the pressure increases up to 44 GPa, the IAD value increases to the maximum at ~ 5.5 GPa and then decreases gradually to a low spin state at ~ 40 GPa, indicating the local moment that the Fe²⁺ is quenched at a critical pressure. At low spin state Fe²⁺, the S equals zero with IAD = 0 (relativity).

The high-pressure electronic transport properties of Ba₉Fe₃Te₁₅ samples were measured through four-probe electrical conductivity methods in DACs made of CuBe alloy. The diamond culet was 300 μm in diameter. The Au wires with a diameter of 18 μm were used as electrodes. A T301 stainless steel gasket was compressed from thickness of 250 μm to 40 μm, and then a hole of 150 μm in diameter was drilled. The cubic BN as an insulating layer was pressed into this hole. A small central hole with diameter of 100 μm was further drilled to serve as the sample chamber, where NaCl fine powder serves as a pressure transmitting medium and a piece of compressed Ba₉Fe₃Te₁₅ powder sample with dimensions of 90 μm × 90 μm × 20 μm was loaded. A ruby ball was loaded simultaneously as a pressure marker. The DAC was placed inside a Maglab system with automatic temperature control. A thermometer

was mounted near the diamond to monitor the temperature.

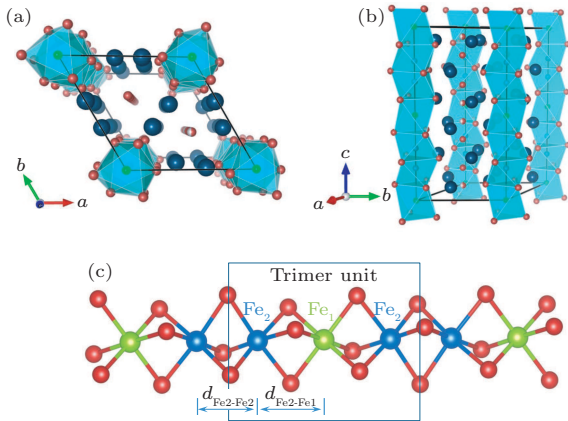


Fig. 1. Schematic diagram of the hexagonal structure in ab -plane (a), along the c axis (b), and individual FeTe_6 chain (the solid line rectangle emphasizes the $-\text{Fe}_2-\text{Fe}_1-\text{Fe}_2$ -trimer) (c). Deep blue balls are barium atoms and red balls are selenium atoms.

The high pressure synthesized $\text{Ba}_9\text{Fe}_3\text{Te}_{15}$ crystallizes into hexagonal structure with the space group of $P-6c2$, as schematically demonstrated in Fig. 1 (refined diffraction under ambient conditions in Fig. S1 of the Supplemental Materials). The face-sharing octahedrons of FeTe_6 stack along the c axis to form a $-\text{Fe}_2-\text{Fe}_1-\text{Fe}_2-$ one-dimensional chain, which is separated by barium ions, as shown in Fig. 1, and the chains are arranged in a triangular geometry. In addition, the distance between the adjacent spin chains is more than 10.2 \AA , expecting a much weak inter-chain coupling. The valence of Fe ions was proved to be $+2$ by the x-ray absorption spectrum.^[7] The magnetic susceptibility data indicated that $\text{Ba}_9\text{Fe}_3\text{Te}_{15}$ is a one-dimensional antiferromagnetic chain exhibiting a hump with the maximum susceptibility at 190 K . The transport property under the ambient condition characterizes $\text{Ba}_9\text{Fe}_3\text{Te}_{15}$ to be a semiconductor with a thermal activation gap $\sim 0.32 \text{ eV}$. Detailed ambient information of $\text{Ba}_9\text{Fe}_3\text{Te}_{15}$ can be found in Ref. [7].

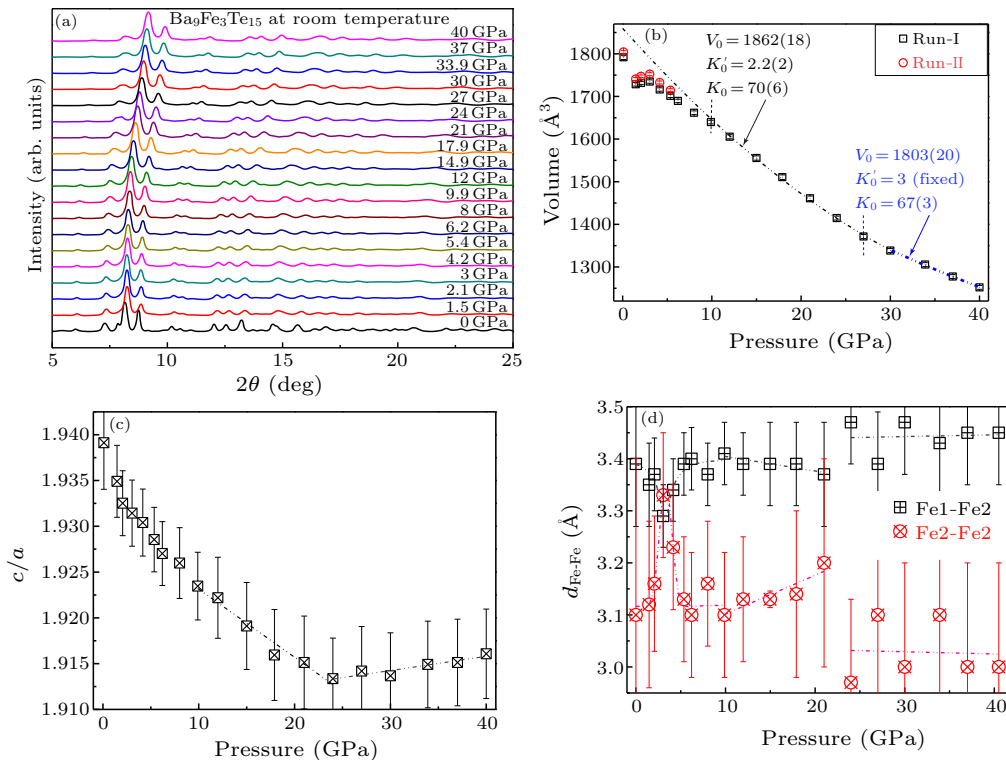


Fig. 2. X-ray diffraction of $\text{Ba}_9\text{Fe}_3\text{Te}_{15}$ collected at HPCAT BM-D with wavelength of 0.4246 \AA and pressure up to 40 GPa, without pressure media used during the experiment (a); volume evolution as a function of pressure, with run I derived from (a), and run II collected at CHESS, Cornell University at wavelength of 0.4863 \AA to double check the low pressure anomaly (b); c/a ratios evolution (c) and Fe-Fe bond length evolutions (d) of $\text{Ba}_9\text{Fe}_3\text{Te}_{15}$ versus pressure.

There is no crystal structure transition in the pressure range studied up to 40 GPa, as shown in Fig. 2 (representative diffraction refinement at 9.88 GPa is plotted in Fig. S2). However, in the low-pressure region, the volume of $\text{Ba}_9\text{Fe}_3\text{Te}_{15}$, as shown in Fig. 2(b), collapsed upon compressing and, then turned to ab-

normal increase with pressure up to 3 GPa and further decreased, showing a dome shape feature. This volume evolution indicated complex spin/charge fluctuation driven by the compression of hexagonal lattice, especially from compression of the FeTe_6 chain along the c axis. The resulted Fe_1/Fe_2 distribution

and distortion of $\text{Fe}_1\text{Te}_6/\text{Fe}_2\text{Te}_6$ octahedrons are plotted in Fig. 2(d). More specifically, the homogenized Fe 1D framework at ~ 3 GPa, which means that the $\text{Fe}_1\text{-Fe}_2$ bond and $\text{Fe}_2\text{-Fe}_2$ bond have the same lengths, is close to the hypothetical un-trimerized unit cell of Ba_3FeTe_5 . The trimerization will result in shorter and longer iron bonds and distorted FeTe_6 octahedrons, therefore quenched some high spin (HS) state into low spin (LS) of Fe^{2+} in FeTe_6 octahedron. Interestingly, compression initially “suppressed” the trimerization and lattice distortion to an end at ~ 3 GPa, resulting in high spin state and overall volume expansion. As the anomaly of the volume at low pressures, the equation of state (EoS) only used the data higher than 10 GPa.

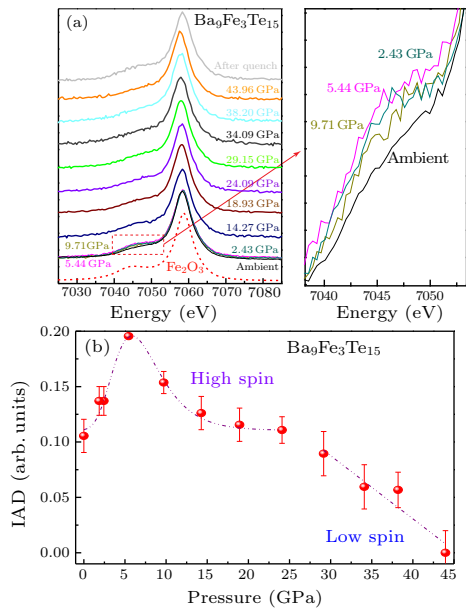


Fig. 3. XES of Fe-K_β and $\text{Fe-K}'_\beta$ edges for $\text{Ba}_9\text{Fe}_3\text{Te}_{15}$ as a function of pressure up to 44 GPa, with $\alpha\text{-Fe}_2\text{O}_3$ used as reference of high spin state, and the right panel enlarged the pre K'_β edges at low pressure region (a); IAD values as a function of pressure, obtained relative to the low spin spectra of $\text{Ba}_9\text{Fe}_3\text{Te}_{15}$ at 44 GPa (b).

For elaboration of the proposed spin state transition in $\text{Ba}_9\text{Fe}_3\text{Te}_{15}$, XES was performed as a function of pressure. As shown in Fig. 3, all spectra show a main peak located at 7058 eV, referred to as $\text{Fe K}_{\beta 1,3}$ lines and a satellite peak located at 7045.5 eV, denoted as $\text{K}_{\beta'}$. XES of Fe ions under high pressure can give the evolution of local spin states, such as low-spin, high-spin and intermediate-spin (IS) states. For better characterizing the initial spin state at ambient pressure, Fe_2O_3 was used as the reference material for HS, as the dashed plots in Fig. 3(a). The satellite peak around 7045.5 eV, mainly derived from exchange interaction between the core hole and 3d magnetic moment, is pronounced characteristic of the HS state.^[22] As described by Peng *et al.*,^[23] the satellite peak is expected to shrink and move closer to the main peak with decreasing 3d magnetic moment as the applied

pressure increases. Generally, the spin state transition from HS to LS is often realized with increasing pressure. Surprisingly, the above experimental observation in Fig. 3(b) suggested that the Fe 3d magnetic moment changes from an “IS state” to an HS state with increase of pressure to 5.5 GPa, and gradually collapses, resulting in an overall LS state at pressure of 44 GPa. The family compound $\text{Ba}_9\text{Fe}_3\text{Se}_{15}$ gives a full HS state at ambient pressure. The pressure driven HS state is unusual and tightly related to crystal structural parameters, such as distortion and rotation of FeTe_6 octahedron. Generally, the Fe^{2+} with $3d^6$ can be either LS or HS, but never be IS in octahedron symmetry. Considering the trimerization of $\text{Ba}_9\text{Fe}_3\text{Te}_{15}$ at ambient pressure, the initial spin state should be a hybridization of LS/HS states of Fe^{2+} ions in two different FeTe_6 octahedrons. As mentioned above, the trimerization was fully suppressed at ~ 3 GPa, leaving only the HS state of Fe^{2+} ions in an identical octahedral chemical environment. In general, the spin state of a given transition metal ion depends on the competition of the crystal field splitting energy ($10Dq$) and the electronic Coulomb repulsion or exchange interaction in a Hubbard model. As an intra-atomic property, the exchange interaction is barely affected by pressure in contrast to the crystal field energy, which is severely determined by interatomic distance and hence by pressure. Thus, magnetic collapse occurs, when the crystal field splitting strength overcomes the magnetic exchange. The high spin state of Fe^{2+} with $e_g^2 t_{2g}^4$ electron configuration stabilized by Hutt’s rule is replaced by low spin state with $e_g^0 t_{2g}^6$ electron configuration under a high pressure condition, leading to the ionic radius decrease of Fe^{2+} from 0.78 Å to 0.61 Å and hence unit volume contraction.^[24] The LS state gains more energies than the HS state due to the increase of $10Dq$. The HS-to-LS transition is then understood as resulting from the conjugated effects of increase of the crystal-field parameter $10Dq$ and a broadening of the Te-5p bandwidth, together with an increasing covalent contribution from the hybridization to the ligand field at high pressure. In the case of $\text{Ba}_9\text{Fe}_3\text{Te}_{15}$, the homogenized irons along the *c* direction and less distortion of the FeTe_6 octahedron at ~ 3 GPa will reduce the crystal field splitting energy, therefore favoring HS state. Further increasing pressure will enhance the distortion and crystal field splitting strength, eventually leading to the LS state. The behavior changes of pressure-dependent spin evolution at ~ 25 GPa, could be possibly related to the dimensional change of electrons, which will be discussed in the following.

Further increasing the pressure, an inconspicuously discontinuous change (as the results cannot be well fitted by single EoS in the whole pressure range) of volume happened approximately at pressure of 25 GPa to 30 GPa. The anomaly indicated a possible electronic structural transition, other than crystal structure transition, as shown in Fig. 2(b), which is

quite similar with the results of $\text{Ba}_9\text{Fe}_3\text{Se}_{15}$.^[9] This anisotropic compression and c/a ratio anomaly at ~ 21 to 25 GPa [shown in Fig. 2(c)] may lead to micro environmental change of FeTe_6 octahedron. In the low-pressure region, the c axis is the easy compression direction, while at pressure higher than 25 GPa, the a axis has similar compressibility as the chain direction, indicating that electronic interaction among different chains enhanced, resulting an electronic re-configuration and a possible 1D-3D electronic phase transition. As observed in the system of La_3TiX_5 (X denotes P, As and Sb), which host similar hexagonal crystal structure with interchain distance of 9–10 Å, the research results show that the La^{3+} ions between the interchain sites are not perfectly ionic and bridge the conducting chains to cause the 3D metallic behavior.^[25] In addition, the electronic transport along 1D chain is easily broken due to the Umklapp scattering as observed in Ba_3TiTe_5 .^[5] Therefore, it is reasonable concluded that the electron transfer among the interchains in $\text{Ba}_9\text{Fe}_3\text{Te}_{15}$ may be realized by Ba^{2+} located at the interstitial site due to the more extended $5p$ valence band and $3d$ band under pressure. Meanwhile, the suddenly jump of $\text{Fe}_1\text{—Fe}_2/\text{Fe}_2\text{—Fe}_2$ bond length at the exact pressure [shown in Fig. 2(d)] indicated that new bonds form among individual chains in the 3D electronic framework.

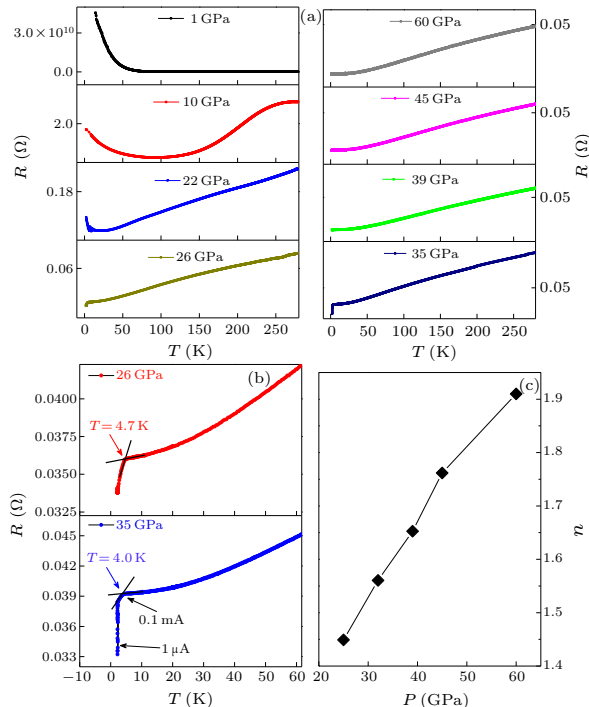


Fig. 4. (a) Electronic transport property of $\text{Ba}_9\text{Fe}_3\text{Te}_{15}$ polycrystalline sample as functions of pressure and temperature; (b) the enlarged view of resistance at 26 GPa and 35 GPa; (c) the pressure dependence of exponent in the range of 25–60 GPa.

Considering the redistribution of electrons and its influence on the electronic transport property, resistance as functions of pressure and temperature was

collected, as shown in Fig. 4, as well as in Fig. S3. The temperature-dependent resistance at 2.6 GPa and 6.0 GPa show a similar semiconductor behavior and with a more pronounced U-shape line at 4.0 GPa in between, suggesting electronic/spin state reentrance (Fig. S3). While further increasing the pressure, the insulating state of $\text{Ba}_9\text{Fe}_3\text{Te}_{15}$ is partially suppressed, and more importantly, there is an insulator-to-metal (MIT) transition occurring at ~ 8 GPa, coinciding with the structural anomaly [Fig. 2(b)] and the HS-to-LS transition [Fig. 3(b)]. The pressure-driven decrease of interatomic distance between Fe and Te can affect the orbital overlap and the related bandwidth for bandwidth-control metal insulator transition. Compared with Mott transition, where $3d$ electron hops from one transition metal ion to another, a charge-transfer insulator was proposed by Zaanen, Sawatzky and Allen (ZSA) in 1985, in which the minimum energy exciting an electron from the anion valence band to the transition-metal d band is referred to as charge-transfer gap.^[26] The transition-metal dihalides, such as NiI_2 , CoI_2 and FeI_2 , have been studied comprehensively under pressure as charge-transfer insulator. Upon increasing pressure, the p - d hybridization strength increases.^[27] Eventually, a first-order MIT occurs depending on the strength of the p - d interaction.^[28] In the $\text{Ba}_9\text{Fe}_3\text{Te}_{15}$ system, charge transfer from the Te $5p$ valence band to the Fe $3d$ band is proposed as the principal mechanism responsible for the MIT transition. The full metallization of $\text{Ba}_9\text{Fe}_3\text{Te}_{15}$ occurred at pressure above 22 GPa, consistent with the structural parameter anomaly and spin state sharp changes at similar pressure. Finally, at 26 GPa a down-shape dropping of the resistance occurred, indicating a superconductivity transition at ~ 4.7 K. The above observations are quite like the high-pressure resistance behaviors in BaFe_2S_3 and BaFe_2Se_3 , where superconductivity was induced by compression. Similar to quasi-1D spin ladder BaFe_2S_3 , in which electrons transfer from S to Fe,^[15] in our study charges transfer from Te to Fe in $\text{Ba}_9\text{Fe}_3\text{Te}_{15}$, i.e., the so-called self-doping mechanism of induced superconductivity at high pressure. It has tentatively interpreted the magnetism and superconducting by the local moment approach^[29–32] in both iron-based and cuprate materials. The superconductivity persists at 35 GPa with a T_c at ~ 4 K and vanishes at higher pressure as shown in Fig. 4. The absence of zero resistance could be due to technical limitations inherent in the experimental apparatus, such as non-hydrostatic compression inside the DAC. It is noting that high-pressure experimental trials using the DAC were performed for samples 1 and 2 in Fig. 4 and Fig. S3, which leads to similar resistance behavior. The superconductivity transition persists from 32 GPa to 60 GPa for sample 2 (Fig. S3) and shows some overlapping pressure range to sample 1 (Fig. 4). In addition, XES experiments show the local spin of

Fe^{2+} fully collapses at 40 GPa. That is, all electrons are paired in Fe^{2+} ions with a low spin state. Thus, it seems not compatible with the metallic state in the electronic transport under high pressure conditions. However, it is worth noting that the orbital hybridization between transition metal ions and coordinated ions plays more and more important role on the transport property with pressure increasing. Thus, the electronic transport property is more dependent on the p - d hybridization strength in $\text{Ba}_9\text{Fe}_3\text{Te}_{15}$. Herein, we conclude that Fe and Te, even Ba ions together contribute to the metallic property at high pressure even though Fe^{2+} with a low spin state. The normal state of resistance between 20 and 100 K in the range of 25 to 60 GPa is fitted by the formula $R = R_0 + AT^n$, where R_0 is the residual resistance, A is the coefficient of the power law, and n is the exponent. The obtained exponent n dependent on pressure is plotted in Fig. 4(c), which shows that n increases from 1.43 to 1.92 as the pressure increases, i.e., the system develops from a non-Fermi liquid (NFL) to a Fermi liquid (FL) state. Therefore, the gradual decrease in the MIT temperature associated with a spin transition from high spin to low spin may suggest a quantum critical point, after which the normal state in metal region changes from NFL to FL. To further demonstrate the crossover from a non-FL to an FL state, the temperature- and pressure-dependent exponent in the metallic region is plotted in Fig. 5, where the color shading represents the value of the exponent n . Figure 5 is a summarized pressure-temperature phase diagram of $\text{Ba}_9\text{Fe}_3\text{Te}_{15}$ including MIT, NFL-to-FL transition, and superconductivity.

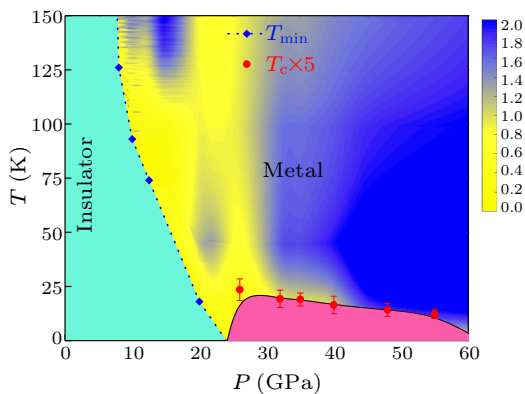


Fig. 5. The pressure and temperature phase diagram of $\text{Ba}_9\text{Fe}_3\text{Te}_{15}$. The MIT, NFL-to-FL transition, superconductivity all are included.

Under ambient conditions, the $\text{Ba}_9\text{Fe}_3\text{Te}_{15}$ is a 1D bandwidth-control-type charge-transfer insulator with a mixed spin state. As the pressure increased to 3–6 GPa, compression of the FeTe_6 chain along c axis resulted in Fe_1/Fe_2 redistribution and convergence of $\text{Fe}_1\text{Te}_6/\text{Fe}_2\text{Te}_6$ octahedrons, which was unambiguously reflected by the spin state evolving from the mixed spin to the HS state. Further, the pres-

sure induced metal-insulator transition emerged at 8 GPa with crossover temperature $T_{\min} \sim 130$ K, and gradually suppressed to be complete metallic phase above 22 GPa, is driven by charge-transfer gap closure in $\text{Ba}_9\text{Fe}_3\text{Te}_{15}$ as a charge-transfer insulator. The unusual exponent n change near 15 GPa, above 125 K was observed, which originated from unstable n change caused by the metal-insulator crossover. The MIT denotes that the electronic structure gradually evolves from 1D to high dimension. The superconductivity started at 26 GPa, accompanied by entering high dimensional metal region and gradually collapsed spin moment, and persisted to 60 GPa in a nonmagnetic state. The hexagonal (1D) crystal of $\text{Ba}_9\text{Fe}_3\text{Te}_{15}$ offers an ideal framework and system for studying the dimensional change and correspondingly physics properties evolution, such as the crystal distortion driven spin state change, magnetic collapse, the MIT and eventually superconductivity emerging as a function of pressure.

References

- [1] Sun J P, Matsuura K, Ye G Z, Mizukami Y, Shimozawa M, Matsubayashi K, Yamashita M, Watashige T, Kasahara S, Matsuda Y, Yan J Q, Sales B C, Uwatoko Y, Cheng J G and Shibauchi T 2016 *Nat. Commun.* **7** 12146
- [2] Wu H, Zhou Y H, Yuan Y F, Chen C H, Zhou Y, Zhang B W, Chen X L, Gu C C, An C, Wang S Y, Qi M Y, Zhang R R, Zhang L L, Li X J and Yang Z R 2019 *Chin. Phys. Lett.* **36** 107101
- [3] Liu Z Y, Dong Q X, Shan P F, Wang Y Y, Dai J H, Jana R, Chen K Y, Sun J P, Wang B S, Yu X H, Liu G T, Uwatoko Y, Sui Y, Yang H X, Chen G F and Cheng J G 2020 *Chin. Phys. Lett.* **37** 047102
- [4] Pouget J P, Regnault L P, Ain M, Hennion B, Renard J P, Veillet P, Dhaleenne G and Revcolevschi A 1994 *Phys. Rev. Lett.* **72** 4037
- [5] Zhang J, Jia Y, Wang X, Li Z, Duan L, Li W, Zhao J, Cao L, Dai G, Deng Z, Zhang S, Feng S, Yu R, Liu Q, Hu J, Zhu J and Jin C 2019 *NPG Asia Mater.* **11** 11
- [6] Zhang J, Wang X C, Adroja D T, Silva I d, Khalyavin D, Sannigrahi J, Nair H S, Duan L, Zhao J F, Deng Z, Yu R Z, Shen X, Yu R C, Zhao H, Zhao J M, Long Y W, Zhu J L, Hu Z W, Lin H J, Chen C T, Wu W and Jin C Q 2020 (submitted)
- [7] Zhang J, Duan L, Wang Z, Wang X, Zhao J, Jin M, Li W, Zhang C, Cao L, Deng Z, Hu Z, Agrestini S, Valvidares M, Lin H J, Chen C T, Zhu J and Jin C 2020 *Inorg. Chem.* **59** 5377
- [8] Zhang J, Liu M, Wang X C, Zhao K, Li W M, Duan L, hao J F, Cao L P, Dai G Y, Deng Z, Zhang S J, Feng S M, Liu Q Q, Yang Y F and Jin C Q 2018 *J. Phys.: Condens. Matter* **30** 214001
- [9] Zhang J, Hao Y, Wang X, Liu M, Yang Y, Duan L, Jin M, Li W, Zhao J Z, Cao L, Deng Z, Zhu J and Jin C 2020 (submitted)
- [10] Koga A 2002 *Phys. Lett. A* **296** 243
- [11] Nakamura H, Yamasaki T, Giri S, Imai H, Shiga M, Kojima K, Nishi M, Kakurai K and Metoki N 2000 *J. Phys. Soc. Jpn.* **69** 2763
- [12] Kelber J, Aldred A T, Lander G H, Mueller M H, Massenet O and Stucky G D 1980 *J. Solid State Chem.* **32** 351
- [13] Gauzzi F L A, Barisic N, Calestani G L, Bolzoni F, Gilioli E, Marezio M, Sanna A, Franchini C and Forro L 2003 *Int. J. Mod. Phys. B* **17** 3503

- [14] Yamasaki T, Nakamura H and Shiga M 2000 *J. Phys. Soc. Jpn.* **69** 3068
- [15] Graf T, Mandrus D, Lawrence J M, Thompson J D, Canfield P C, Cheong S W and Rupp L W 1995 *Phys. Rev. B* **51** 2037
- [16] Forro L, Gaal R, Berger H, Fazekas P, Penc K, Kezsmarki I and Mihaly G 2000 *Phys. Rev. Lett.* **85** 1938
- [17] Takahashi H, Sugimoto A, Nambu Y, Yamauchi T, Hirata Y, Kawakami T, Avdeev M, Matsubayashi K, Du F, Kawashima C, Soeda H, Nakano S, Uwatoko Y, Ueda Y, Sato T J and Ohgushi K 2015 *Nat. Mater.* **14** 1008
- [18] Yamauchi T, Hirata Y, Ueda Y and Ohgushi K 2015 *Phys. Rev. Lett.* **115** 246402
- [19] Ying J, Lei H, Petrovic C, Xiao Y and Struzhkin V V 2017 *Phys. Rev. B* **95** 241109
- [20] Larson A C and Dreele R B V O N 2000 *Los Alamos National Laboratory Report Laur 86*
- [21] Vankó G, Neisius T, Molnár G, Renz F, Kárpáti S, Shukla A and de Groot F M F 2006 *J. Phys. Chem. B* **110** 11647
- [22] Rueff J P and Kao C C 1999 *Phys. Rev. Lett.* **82** 3284
- [23] Peng G, Wang X, Randall C R, Moore J A and Cramer S P 1994 *Appl. Phys. Lett.* **65** 2527
- [24] <http://abulafia.mt.ic.ac.uk/shannon/ptable.php>
- [25] Duan L, Zhang J, Wang X, Zhao J, Cao L, Li W, Deng Z, Yu R, Li Z and Jin C 2020 *J. Alloys Compd.* **831** 154697
- [26] Zaanen J, Sawatzky G A and Allen J W 1985 *Phys. Rev. Lett.* **55** 418
- [27] Chen A 1993 *PhD Thesis* (University of California)
- [28] Giesekeus A and Falicov L M 1991 *Phys. Rev. B* **44** 10449
- [29] Si Q and Abrahams E 2008 *Phys. Rev. Lett.* **101**
- [30] Yu R and Si Q M 2013 *Phys. Rev. Lett.* **110** 146402
- [31] de' Medici L, Giovannetti G and Capone M 2014 *Phys. Rev. Lett.* **112** 177001
- [32] Werthamer N R, Helfand E and Hohenberg P C 1966 *Phys. Rev.* **147** 295